# Fabrication-Tolerant Microstrip Quarter-Wave Stepped-Impedance Resonator Filter

Cheng-Hsien Liang, Chin-Hsiung Chen, and Chi-Yang Chang, *Member, IEEE*

***Abstract*—The etching error causes serious frequency drift of a microstrip stepped-impedance resonator (SIR). This paper proposes a novel microstrip quarter-wave SIR structure, which is insensitive to fabrication tolerances. Inserting several ground strips in the low-impedance section of the resonator keeps the impedance ratio almost constant in spite of inaccurate fabrication. As an additional benefit, the resonator size would be miniaturized because the characteristic impedance of the microstrip line in the low-impedance section is mainly controlled by the signal strips and the inserted ground strips in a coplanar manner. The concepts and characteristics of this modified resonator structure are discussed in detail. The filters constructed by the conventional microstrip SIR were also designed and fabricated at the same frequency band to compare with the proposed ones. Measured results show that each proposed filter has compact size, wide stopband, and high tolerance to fabrication errors. Two four-pole cross-coupled filters were designed and fabricated to demonstrate the feasibility.**

***Index Terms*—Cross-coupled filter, fabrication tolerance, ground strip, spurious response, stepped-impedance resonator (SIR), transmission zero.**

## I. Introduction

HIGH-PERFORMANCE bandpass filters have become more and more important in recent years due to the rapid growth in modern wireless communication systems. The microstrip filter plays an important role in modern filter applications owing to its planar structure and easy integration into the printed circuit board (PCB). Recently, the stepped-impedance resonator (SIR) filter has been a hot topic because of its ability to reduce the circuit size and to improve the upper stopband performance. There are many related studies on SIR filters [1]–[12]. The SIR filters can be categorized into three major types, namely: 1) quarter-wave; 2) half-wave; and 3) one-wavelength SIR filters. Since the $\lambda/4$ SIR has a smaller size and fewer spurious modes than other type of SIRs, it is of great benefit to the design of microstrip bandpass filters.

A conventional $\lambda/4$ microstrip SIR structure is shown in Fig. 1(a) [9]. It comprises a section of high-impedance $(Z_1)$ and a section of a low-impedance $(Z_2)$ transmission line with corresponding physical (electrical) lengths $L_1(\theta_1)$ and $L_2(\theta_2)$, respectively. By adjusting structural parameters, the low- to high-impedance ratio (i.e., $R = Z_2/Z_1$) of the $\lambda/4$ SIR can be changed, which leads to various resonant frequencies. Furthermore, the first spurious frequency can be tuned much higher than the fundamental frequency so that a wide stopband can be achieved to meet requirements. In other words, the impedance ratio $R$ is the most important parameter characterizing the properties of the SIR. Theoretical analysis reveals that the resonator in Fig. 1(a) has a minimum length and a large span between the fundamental and spurious frequencies when the high- and low-impedance sections are equal in length (i.e., $L_1 = L_2$) and $R < 1$ [5], [7], [9]. Hence, in most practical applications, $R$ is chosen as small as possible and $L_1 = L_2$ is preferred.

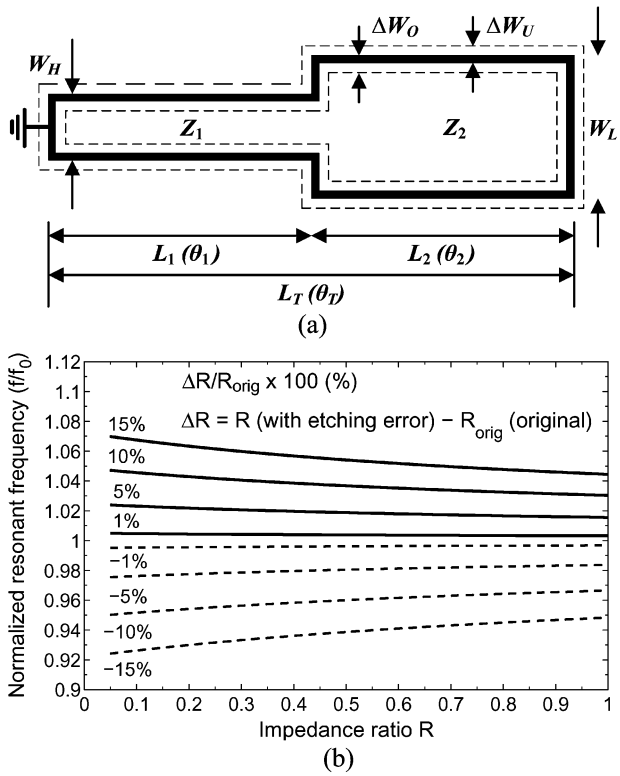


Fig. 1. (a) Conventional $\lambda/4$ microstrip SIR. Dashed lines represent etching errors. (b) Normalized resonant frequency versus the percentage variation of the impedance ratio.

Due to the restriction of the fabrication process, manufacturing tolerances influence the performance of the filter and cause a shift of the center frequency. For a constant amount of etching error, as shown in Fig. 1(a) ($\Delta W_U$ for under-etching and $\Delta W_O$ for over-etching), the percentage width variation (etching error divided by the normal width in percent) in the high-impedance section is much larger than that in the

Manuscript received April 09, 2008; revised October 08, 2008. First published April 14, 2009; current version published May 06, 2009. This work was supported in part by the National Science Council under Grant NSC95-2221-E-009-042-MY3, and by the Ministry of Education (MoE) under an MoE Aiming for the Top University (ATU) Plan Grant.

The authors are with the Department of Communication Engineering, National Chiao Tung University, Hsinchu 300, Taiwan (e-mail: seaman.cm96g@g2.nctu.edu.tw; hsuing@hotmail.com; mhchang@cc.nctu.edu.tw).

Color versions of one or more of the figures in this paper are available online at http://ieeexplore.ieee.org.

Digital Object Identifier 10.1109/TMTT.2009.2017345

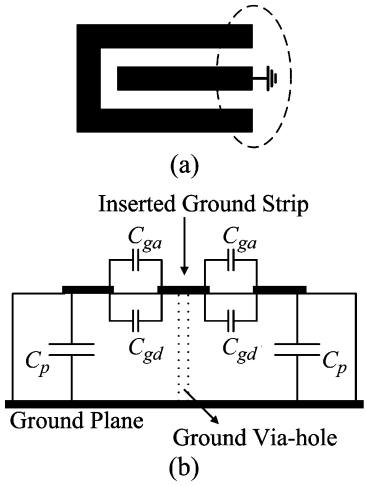


Fig. 2. (a) Top view of the proposed microstrip structure. (b) Cross-sectional view of the circled portion in (a).

low-impedance section. Thus, the variation of the characteristic impedance of the high-impedance line is different from that of the low-impedance line, and this causes the impedance ratio to change.

The normalized resonant frequency versus the percentage variation of the impedance ratio $R$ is shown in Fig. 1(b), where different curves correspond to different amounts of variation in $R$ due to etching errors. It is observed that small changes in the impedance ratio would contribute to obvious variations in the resonant frequency. As an example, consider two conventional $\lambda/4$ microstrip SIRs, shown in Fig. 1(a), with different physical dimensions on the substrate with a dielectric constant of 3.6 and a thickness of 0.5 mm. The first case is $W_H = 0.225$ mm and $W_L = 3.45$ mm, which corresponds to $R = 0.204$. The second case is $W_H = 1.25$ mm and $W_L = 1.45$ mm, which corresponds to $R = 0.906$. For $\Delta W_O = 0.025$ mm (i.e., over-etching 0.05 mm), the impedance ratio $R$ is changed to 0.189 for the first case and to 0.904 for the second case. The percentage variations of the impedance ratio $R$ for the first and second cases due to the over-etching are $-7.35\%$ and $-0.22\%$, respectively. As a result, the first case would have $-3.334\%$ of the frequency drift, and the second case would only have $-0.073\%$ of the frequency drift. The frequency drift due to etching errors becomes larger as the impedance ratio becomes smaller. Therefore, the conventional microstrip SIR structure is very sensitive to fabrication tolerances such as over-etching, under-etching, and errors in substrate thickness. Sometimes the filter requires a substantial amount of tuning and even additional iteration to meet the desired performance specification. Although numerous studies have been performed on the advantages of SIRs [1]–[12], how to decrease the effect of fabrication tolerances is still critically lacking.

As mentioned above, the fabrication tolerance is an important factor in filter design, especially for the SIR case. In this paper, a novel $\lambda/4$ microstrip SIR structure with inserted ground strips is proposed. In the modified structure, the ground strip is only placed on the signal plane of the low-impedance section. This method will increase the coplanar capacitance and make the characteristic impedance less sensitive to the variation of the substrate thickness. It will be shown later that this

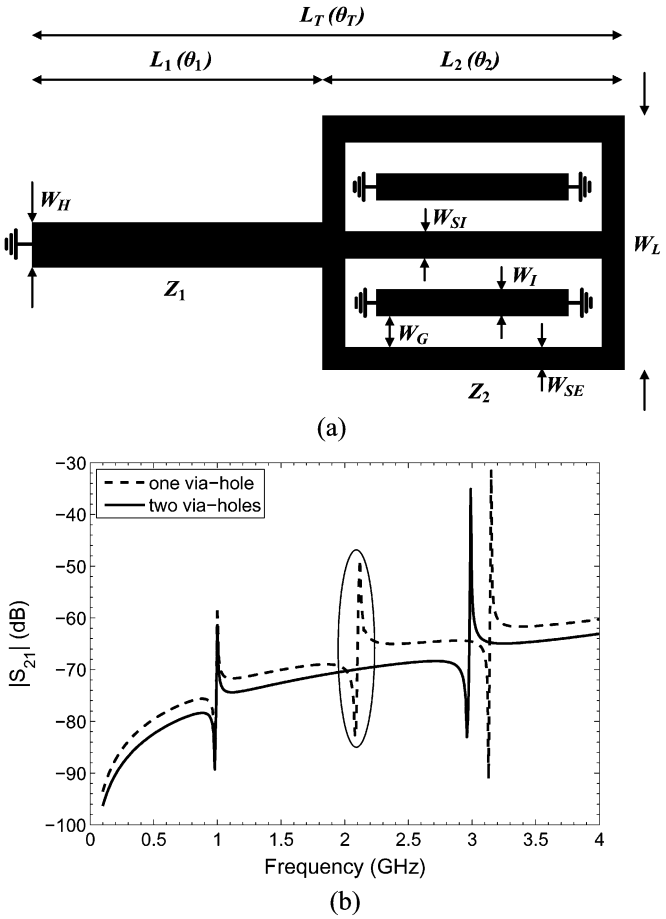


Fig. 3. (a) Proposed $\lambda/4$ microstrip SIR. (b) Comparison of the frequency responses of the resonators with one and two via-holes on the ends of each inserted ground strip.

structure also has a high tolerance for inaccurate fabrication. In addition, the ground strip provides an extra benefit to decrease the characteristic impedance of the low-impedance section so that the resonator length could be shortened. Based on the proposed SIR structure, two compact microstrip cross-coupled bandpass filters with good stopband rejection and excellent tolerance of fabrication errors were designed and fabricated. Here, we use four-pole filters with the cross coupling between resonators 1 and 4 as examples. Both filters use the tapped-line input/output structure [13] to save space. To compute the characteristic impedance of the modified microstrip structure, a commercial full-wave electromagnetic (EM) simulator is used.

## II. New Modified Microstrip Structure and Characteristics of the Proposed $\lambda/4$ SIR

Fig. 2 shows the top and cross-sectional views of the proposed microstrip structure. This structure is based on the conventional microstrip line where a ground strip is inserted in the signal plane and a ground via-hole is used. In Fig. 2(b), $C_p$ denotes the parallel-plate capacitance between the signal strip and the microstrip ground plane; $C_{ga}$ and $C_{gd}$ represent the fringe capacitances across the gap between the signal strip and the inserted ground strip in the air and dielectric regions, respectively. While the capacitance $C_p$ diminishes due to the inserted ground strip, however, the capacitances $C_{ga}$ and $C_{gd}$ can compensate for the

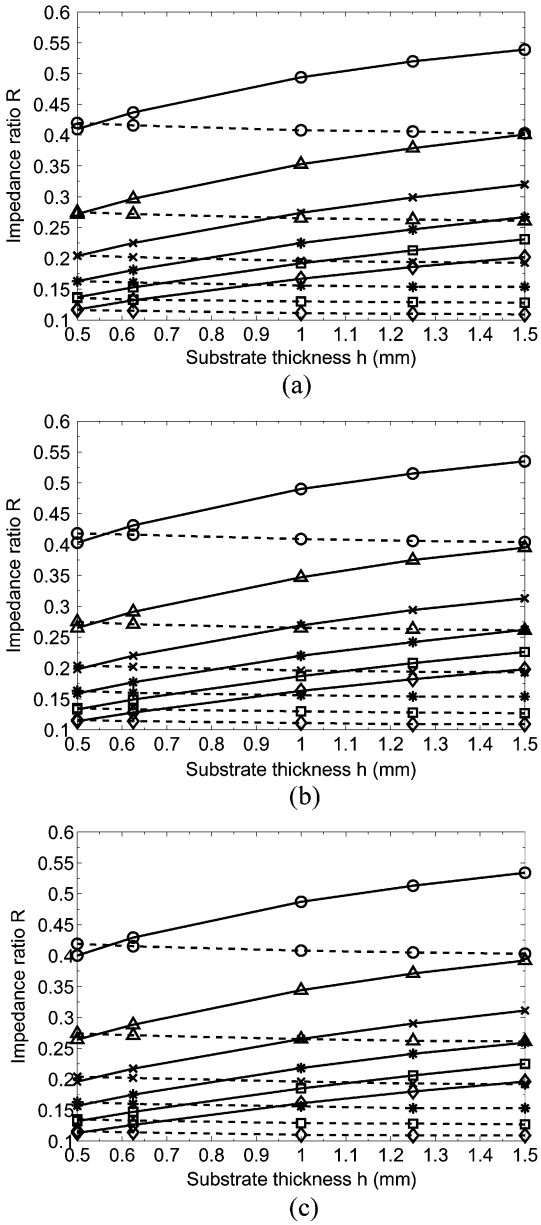


Fig. 4. Impedance ratio $R$ of the conventional and proposed $\lambda/4$ SIRs versus substrate thickness $h$ and width $W_L$ (in millimeters) for: (a) $\epsilon_r = 3.6$, (b) $\epsilon_r = 6.8$, and (c) $\epsilon_r = 10.2$. Conventional: solid line. Proposed: dashed line. (circle $\circ$: $W_L = 1.35$, $N = 1$; triangle $\triangle$: $W_L = 2.4$, $N = 2$; cross $\times$: $W_L = 3.45$, $N = 3$; asterisk $*$: $W_L = 4.5$, $N = 4$; square $\square$: $W_L = 5.55$, $N = 5$; diamond $\diamond$: $W_L = 6.6$, $N = 6$.)

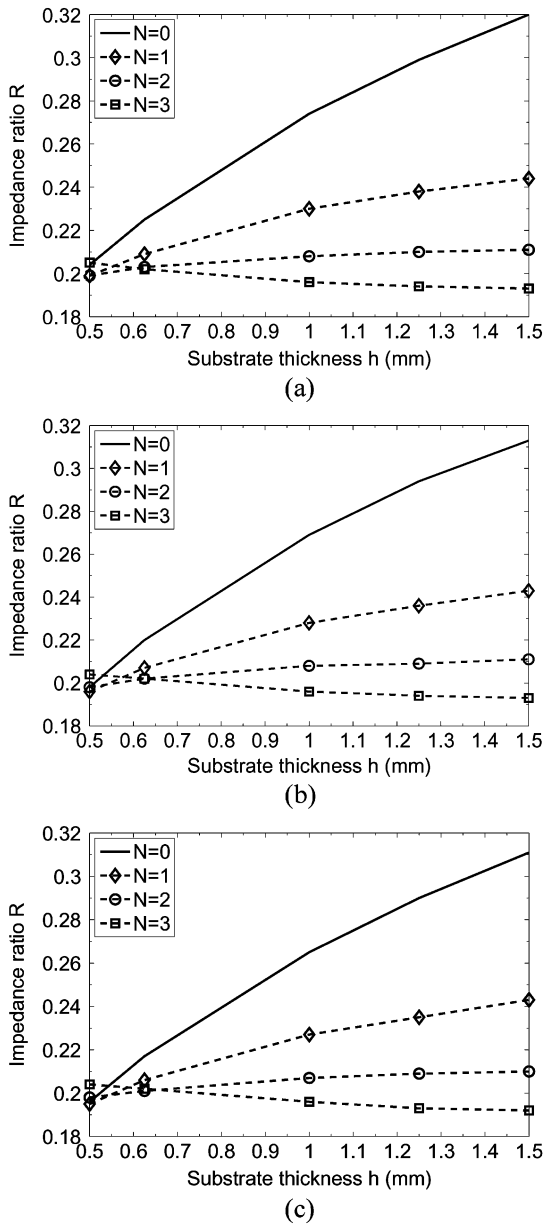


Fig. 5. Impedance ratio $R$ versus substrate thickness $h$ for the proposed $\lambda/4$ SIRs with different numbers of inserted ground strips when $W_L = 3.45$ mm. (a) $\epsilon_r = 3.6$. (b) $\epsilon_r = 6.8$. (c) $\epsilon_r = 10.2$. ($N$: number of inserted ground strips. $N = 0$: conventional microstrip structure.)

decrease of $C_p$. Furthermore, if the strip spacing is small enough compared with the substrate thickness, $C_{ga}$ and $C_{gd}$ become large, which effectively decreases the characteristic impedance. This concept could be used to minimize the resonator size if the lower characteristic impedance is needed, especially for the thick substrate.

On the basis of the structure in Fig. 2(a), more parallel strips can be added to change the characteristic impedance of the microstrip line. Fig. 3(a) shows the proposed $\lambda/4$ microstrip SIR structure. It is seen in the figure that the high-impedance $(Z_1)$ and low-impedance $(Z_2)$ sections are cascaded together and the high-impedance section is short-ended. In comparison with the conventional $\lambda/4$ microstrip SIR structure shown in Fig. 1(a), the proposed one has ground strips in its low-impedance section. The high-impedance section has a physical (electrical) length of $L_1(\theta_1)$ and a width of $W_H$. The low-impedance section has a physical (electrical) length of $L_2(\theta_2)$ and a total width of $W_L$. The total physical (electrical) length of the resonator is $L_T(\theta_T)$. In the low-impedance section, the width of inserted ground strips is $W_I$, the width of inner signal strips is $W_{SI}$, the width of outmost signal strips is $W_{SE}$, and the spacing between strips is $W_G$. Thus, $W_L = 2N \times W_G + N \times W_I + (N-1) \times W_{SI} + 2 \times W_{SE}$, where $N$ is the number of inserted ground strips. Note that an additional ground via-hole is added on the other end of each inserted ground strip in Fig. 3(a) so as to push the resonant frequency of the ground strip to higher frequency. To understand this better, consider the simple case of

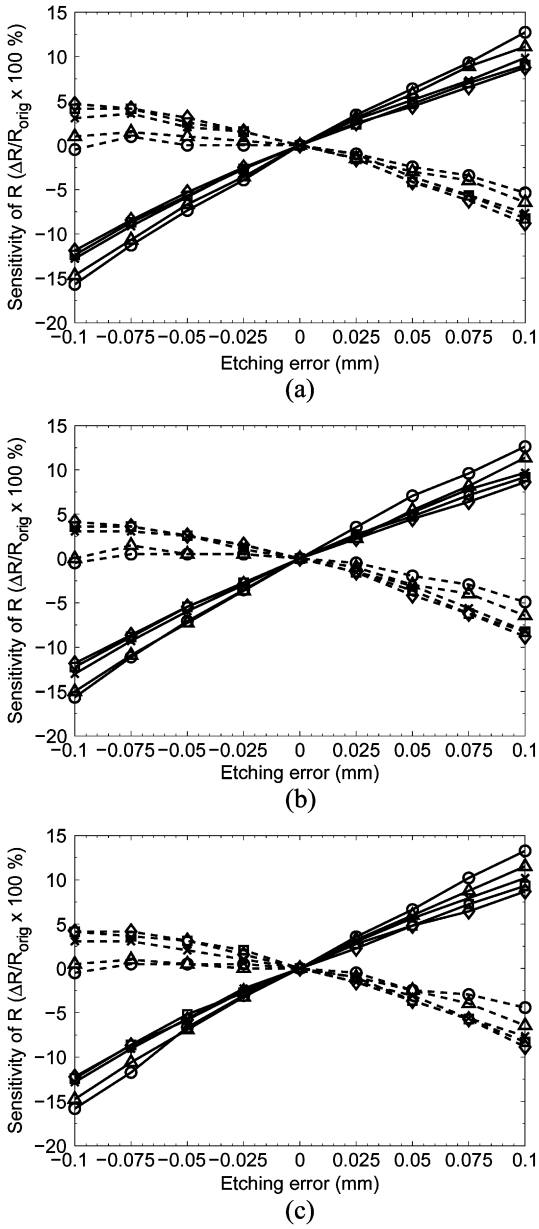


Fig. 6. Sensitivity to etching tolerances for the conventional and proposed $\lambda/4$ SIRs with various values of the substrate thickness $h$ (in millimeters) when $W_L = 3.45$ mm. (a) $\epsilon_r = 3.6$. (b) $\epsilon_r = 6.8$. (c) $\epsilon_r = 10.2$. Conventional: solid line. Proposed ($N = 3$): dashed line. Positive: under-etching. Negative: over-etching. (circle ∘: $h = 0.5$; triangle △: $h = 0.625$; cross ×: $h = 1$; square □: $h = 1.25$; diamond ⋄: $h = 1.5$.)

the resonator with $N = 1$, $L_1 = L_2$, $W_{SE} = W_I = 0.3$ mm, $W_L = W_H = 1.35$ mm, and $W_G = 0.225$ mm on the substrate with a dielectric constant of 3.6 and a thickness of 0.5 mm. Fig. 3(b) compares the frequency responses of two resonators where the inserted ground strips have one via-hole and two via-holes on their ends, respectively. It is apparent that the resonator with two via-holes on the ends of each inserted ground strip has better spurious response.

To compare the characteristics of the proposed $\lambda/4$ SIR with the conventional one, first of all it is necessary to obtain the characteristic impedance of the proposed low-impedance microstrip structure. We first perform the full-wave EM simulation for the proposed microstrip structure by using Sonnet software

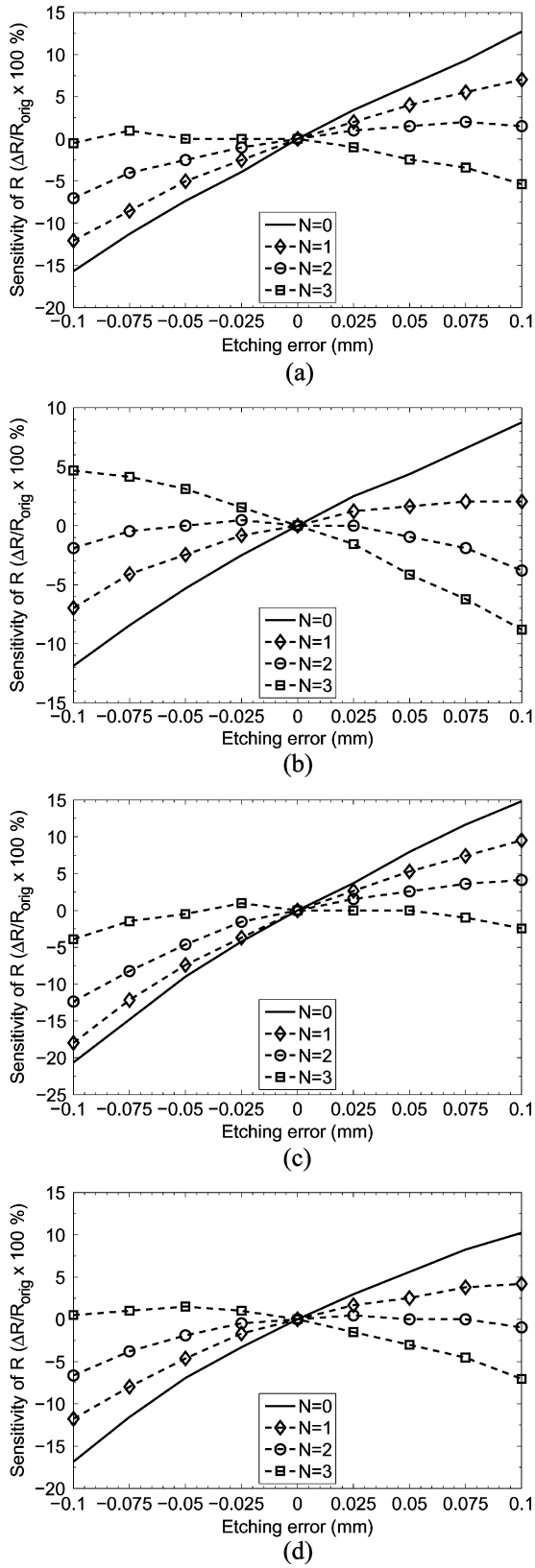


Fig. 7. Sensitivity to etching tolerances for the proposed $\lambda/4$ SIRs with different numbers of inserted ground strips. (Case I: $W_L = 3.45$ mm, $W_{SI} = W_I = 0.3$ mm, and $W_G = W_H = 0.225$ mm. Case II: $W_L = 3.4$ mm, $W_{SI} = W_I = 0.25$ mm, $W_G = 0.275$ mm, and $W_H = 0.175$ mm). (a) Case I: $h = 0.5$ mm. (b) Case I: $h = 1.5$ mm. (c) Case II: $h = 0.5$ mm. (d) Case II: $h = 1.5$ mm. ($N$: number of inserted ground strips. $N = 0$: conventional microstrip structure.)

TABLE I
DESIGN PARAMETERS OF THE PROPOSED SIR FILTERS

| | Filter I | Filter II |
|---|---|---|
| Center frequency $f_0$ (GHz) | 1.02 | 1.02 |
| Bandwidth $\Delta$ | 7% | 10% |
| Impedance ratio $R$ | 0.205 | 0.199 |
| $Q_{ext}$ | 13.697 | 9.58792 |
| $k_{12} = k_{34}$ | 0.0627716 | 0.0896737 |
| $k_{23}$ | 0.0484737 | 0.0692482 |

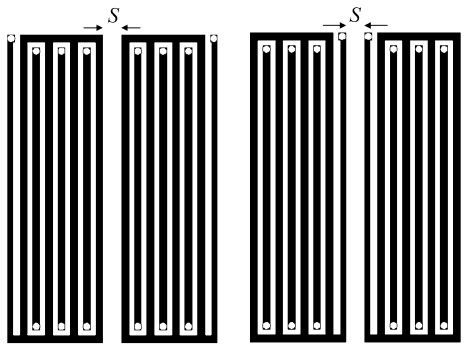


Fig. 8. Coupling structures for: (a) electric coupling and (b) magnetic coupling.

[14], and then load the two-port $S$-parameter file in AWR Microwave Office [15] to obtain the characteristic impedance. A lossless metal is assumed during the simulation. Since the capability of the available fabrication process is taken into account, each via-hole is 0.3 mm in diameter and the following physical dimensions are fixed as $L_1 = L_2$, $W_H = W_G = 0.225$ mm, and $W_{SI} = W_I = 0.3$ mm.

For the same $W_L$ and $W_H$, the impedance ratio $R$ versus substrate thickness $h$ for the conventional and proposed $\lambda/4$ SIRs is shown in Fig. 4 for comparison, where solid lines belong to the conventional SIRs and dashed lines belong to the proposed ones. In Fig. 4, the number of inserted ground strips of the proposed SIRs is maximized so that $W_{SE} = W_{SI} = 0.3$ mm. Thus, different $W_L$ in each figure corresponds to different numbers of inserted ground strips (i.e., from $N = 1$ to 6). Fig. 4(a)–(c) is similar, except substrate dielectric constants $\epsilon_r$ are different. As shown in Fig. 4, it can obviously be found that the impedance ratio $R$ of the proposed SIR is lower than that of the conventional one in most of the substrate thickness values (i.e., $h \geqq 0.57$ mm in all cases). One extra benefit is that the proposed SIR has a nearly constant impedance ratio $R$ versus substrate thickness $h$. The phenomenon implies that the impedance ratio of the proposed SIR is insensitive to the variation of the substrate thickness.

Another interesting issue is about the number of inserted ground strips. As the number of inserted ground strips is not maximized, what will be the performance? Taking $W_L = 3.45$ mm as an example, Fig. 5 depicts the impedance ratio $R$ versus substrate thickness $h$ with the number of inserted ground strips as a parameter. The number $N$ of inserted ground strips is varied from 0 to 3, where $N = 0$ corresponds to the conventional microstrip structure. It is observed that the proposed SIR structure ($N = 1, 2, 3$) is less sensitive to the

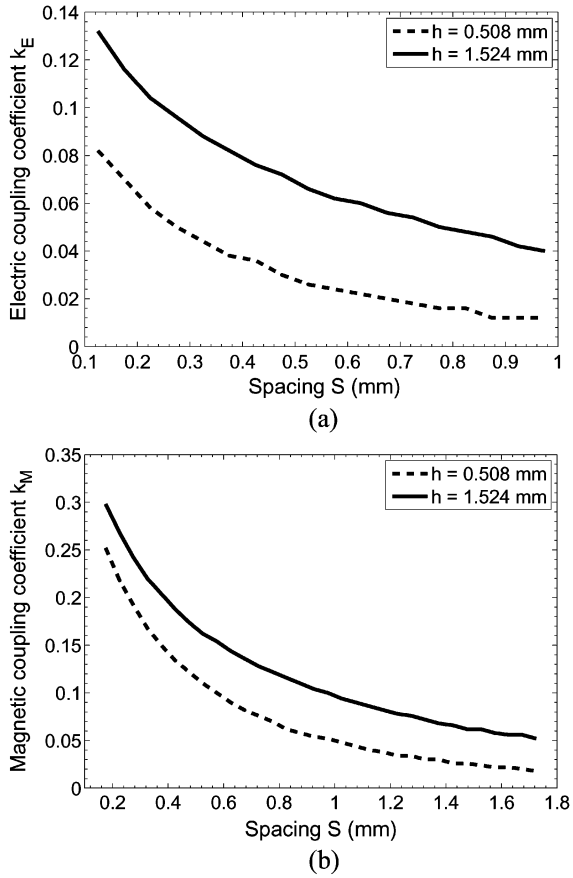


Fig. 9. Coupling coefficients of the coupling structures for: (a) electric coupling and (b) magnetic coupling.

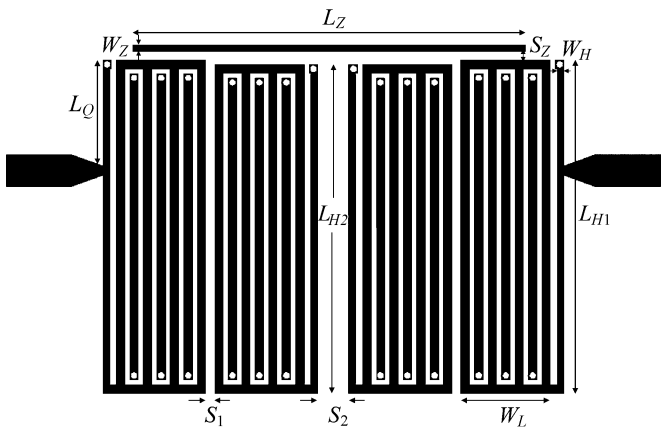


Fig. 10. Proposed layout of the four-pole cross-coupled filter.

substrate thickness variation compared with the conventional one and $N = 2$ or $N = 3$ has the best performance. For the conventional $\lambda/4$ microstrip SIR, the percentage variation of the characteristic impedance of the high-impedance line is much less than that of the low-impedance line under the variation of the substrate thickness. Therefore, the impedance ratio $R$ varies largely for the conventional microstrip SIR structure. The principle behind the proposed $\lambda/4$ microstrip SIR is that in the low-impedance microstrip section, the coplanar signal and ground strips also control the characteristic impedance. As a result, the proposed low-impedance microstrip structure is

TABLE II
DIMENSIONS OF THE DESIGNED FILTERS

| (mm) | $L_{H1}$ | $L_{H2}$ | $W_H$ | $W_{SE}$ | $W_{SI}$ | $W_I$ | $W_G$ | $W_L$ | $L_Q$ | $L_Z$ | $W_Z$ | $S_Z$ | $S_1$ | $S_2$ |
|---|---|---|---|---|---|---|---|---|---|---|---|---|---|---|
| Filter I | 12.925 | 12.75 | 0.225 | 0.3 | 0.3 | 0.3 | 0.225 | 3.45 | 4.125 | 15.225 | 0.225 | 0.175 | 0.175 | 0.925 |
| Filter II | 13.075 | 12.725 | 0.175 | 0.25 | 0.25 | 0.25 | 0.275 | 3.4 | 4.1 | 15.75 | 0.175 | 0.225 | 0.325 | 1.3 |

much less sensitive to the variation of the substrate thickness. Taking Fig. 5(a) as an example, when the substrate thickness $h$ is changed from 0.5 to 1.5 mm, $Z_1$ is changed from 108.4 to 149.7 $\Omega$, and $Z_2$ is changed from 22.1 to 47.9 $\Omega$ for the conventional microstrip structure and from 22.2 to 28.9 $\Omega$ for the proposed one with $N = 3$. Consequently, the impedance ratio $R$ is changed from 0.204 to 0.32 for the $N = 0$ case and from 0.205 to 0.193 for the $N = 3$ case.

During the PCB manufacturing process, the most serious error is the etching error. The over-etching or under-etching occurs frequently from lot to lot. The proposed SIR structure further shows much better tolerance to etching errors than the conventional one. For the case of $W_L = 3.45$ mm in Figs. 4 and 5, Fig. 6 shows the percentage variation of the impedance ratio $R$ of the conventional and proposed $(N = 3)$ $\lambda/4$ SIRs versus etching error (from over-etching 0.1 mm to under-etching 0.1 mm). In each figure, different curves correspond to different substrate thicknesses. Fig. 6(a)–(c) is similar, except substrate dielectric constants $\epsilon_r$ are different. From Fig. 6, it can be clearly observed that the percentage change of the impedance ratio $R$ of the proposed SIR structure is much less than that of the conventional one. The mechanism behind this is that the proposed low-impedance microstrip structure is more sensitive to etching tolerances than the conventional one to keep the impedance ratio unchanged. In other words, for the conventional $\lambda/4$ microstrip SIR, the characteristic impedance variation of the high-impedance line is much larger than that of the low-impedance line under the same amount of etching error, and this causes the impedance ratio to change largely. For example, under the condition of over-etching 0.05 mm and the substrate thickness $h = 0.5$ mm in Fig. 6(a), $Z_1$ is changed 9.13% (from 108.4 to 118.3 $\Omega$), and $Z_2$ is changed 0.9% (from 22.1 to 22.3 $\Omega$) for the conventional microstrip structure. Consequently, $R$ is changed from 0.204 to 0.189 $(\Delta R/R = -7.35\%)$. However, for the proposed low-impedance microstrip structure, $Z_2$ is changed 9.46% (from 22.2 to 24.3 $\Omega$) so that $R$ is almost unchanged $(R = 0.205$ and $\Delta R/R = 0.299\%)$. Here, $W_L = 3.45$ mm is just an example and other $W_L$'s in Fig. 4 also show similar results.

Again, it is interesting to change the number of inserted ground strips. Fig. 7 shows the percentage variation of the impedance ratio $R$ of the proposed $\lambda/4$ SIR versus etching error for different numbers of inserted ground strips. There are two sets of physical dimensions to be used for the simulation. The first one is $W_L = 3.45$ mm, $W_{SI} = W_I = 0.3$ mm, and $W_G = W_H = 0.225$ mm. The second one is $W_L = 3.4$ mm, $W_{SI} = W_I = 0.25$ mm, $W_G = 0.275$ mm, and $W_H = 0.175$ mm. During the simulation, substrates with thicknesses of 0.5 and 1.5 mm and a dielectric constant of 3.6 are used. As shown in Fig. 7, for the given dimensions, the best choice for the number of inserted ground strips can be determined. Taking Fig. 7(a) as an example, $N = 3$ (the maximum allowable number) is the best choice for the first set of dimensions on the given substrate. It is demonstrated that the impedance ratio $R$ of the proposed $\lambda/4$ microstrip SIR is less sensitive to etching tolerances compared with that of the conventional one, even if $N = 1$.

## III. FILTER DESIGN AND SENSITIVITY TO FABRICATION TOLERANCES

To demonstrate the proposed structure, two four-pole cross-coupled bandpass filters were fabricated. The filter adjustment method proposed by Dishal [16] and summarized by Hong and Lancaster [17] is used in our filter design. Since the cross coupling, which produces transmission zeros, is very weak, the initial design procedure is based on the fourth-order Chebyshev response filter with a 0.05-dB equal-ripple passband characteristic. Both filters have the same topology, and their specifications and coupling coefficients are listed in Table I. Filter I was fabricated on a Rogers RO4003 substrate with a relative dielectric constant of 3.58, a loss tangent of 0.0027, and a thickness of 0.508 mm. Filter II was fabricated on the same substrate as filter I, except the thickness is 1.524 mm.

### A. Filter Design

In the design process, we first fix the widths of $W_H$, $W_L$, $W_{SI}$, $W_I$, and $W_G$, and then plot the variation of the impedance ratio versus etching error for different numbers of inserted ground strips. The proper number of inserted ground strips could be chosen for the prescribed dimensions and the available fabrication process.

Fig. 8 shows the two basic coupling structures for our filter design. Note that each SIR is folded for size reduction. There are two kinds of couplings involved in the filter. At resonance, each of the $\lambda/4$ SIRs has the maximum electric fringe fields near the open end and the maximum magnetic fringe fields at the short end. Hence, Fig. 8(a) is for the electric coupling and Fig. 8(b) is for the magnetic coupling. For filter I, the resonator dimensions are $W_L = 3.45$ mm, $W_{SE} = W_{SI} = W_I = 0.3$ mm, and $W_G = W_H = 0.225$ mm. For filter II, they are $W_L = 3.4$ mm, $W_{SE} = W_{SI} = W_I = 0.25$ mm, $W_G = 0.275$ mm, and $W_H = 0.175$ mm. In both filters, the number of inserted ground strips is three. All diameters of via-holes have the same size of 0.3 mm. Based on the structures presented in Fig. 8, the relation between the coupling coefficient and the spacing between adjacent SIRs is shown in Fig. 9.

Fig. 10 depicts the layout of the filters where the physical parameters corresponding to those of Table II are indicated. Here, we number these four resonators as 1–4 from left to right. The coupling $k_{23}$ is magnetic, whereas $k_{12}$ and $k_{34}$ are electric. The source coupling and load coupling are both achieved by a tapped

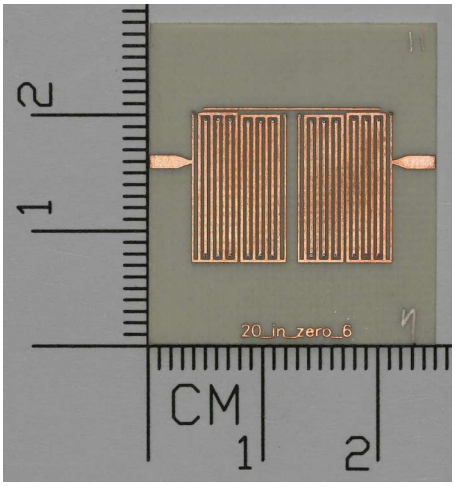


Fig. 11. Photograph of the fabricated circuit (filter I).

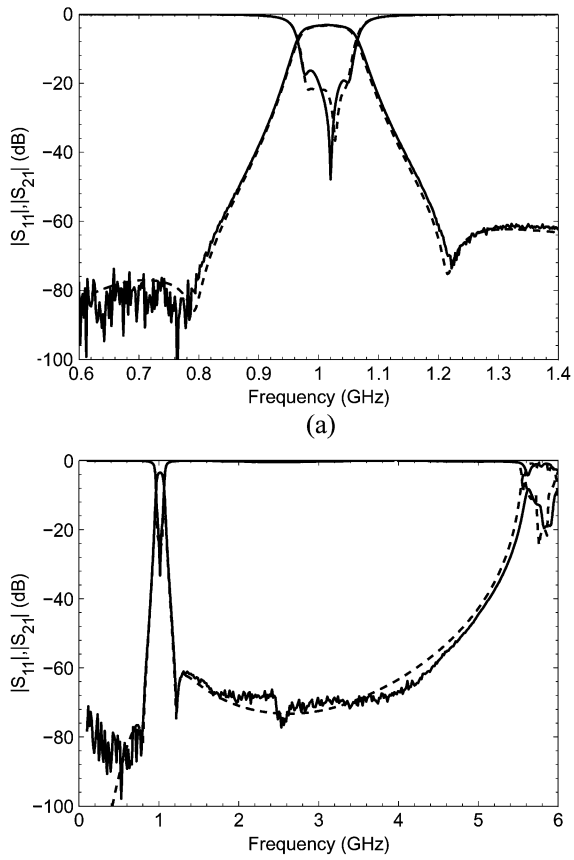


Fig. 12. Simulated (dashed line) and measured (solid line) results ($|S_{11}|$ and $|S_{21}|$) of filter I. (a) Narrowband responses. (b) Wideband responses.

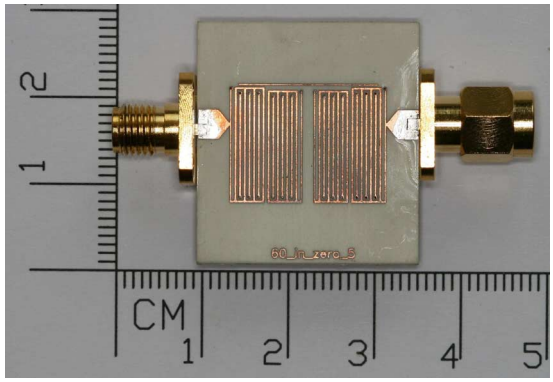


Fig. 13. Photograph of the fabricated circuit (filter II).

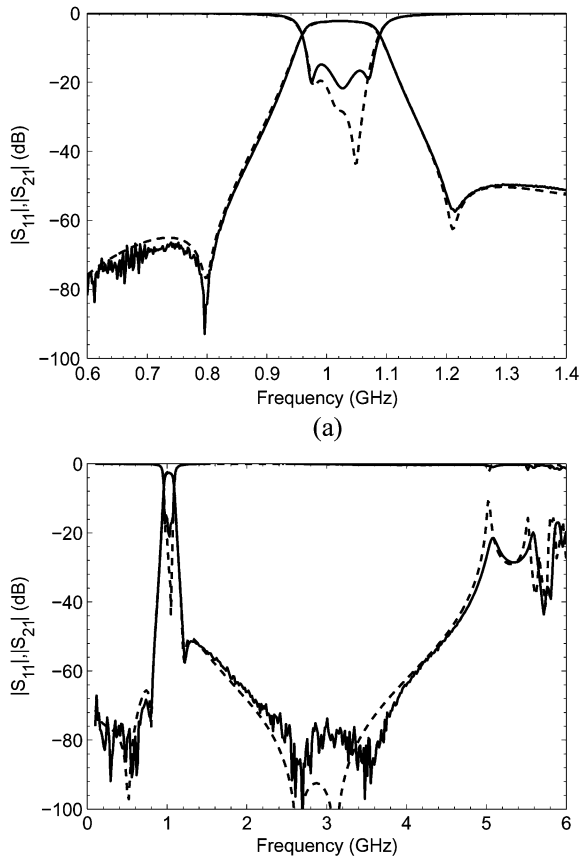


Fig. 14. Simulated (dashed line) and measured (solid line) results ($|S_{11}|$ and $|S_{21}|$) of filter II. (a) Narrowband responses. (b) Wideband responses.

feed line because it is space saving and easy to design [13]. The tap position $L_Q$ is chosen to match the $Q_{\text{ext}}$ value for the 50-$\Omega$ source/load impedance. A thin microstrip line provides the small cross coupling [17], [18] between resonators 1 and 4 to produce a pair of transmission zeros on both sides of the passband. The passband response almost remains unchanged when the cross coupling is applied. The strength of the cross coupling is determined by the length $L_Z$, the width $W_Z$ of the coupling microstrip, and the gap $S_Z$ between the coupling microstrip and resonators 1 and 4. Herein, two transmission zeros are placed at 0.8 and 1.2 GHz. The commercial full-wave EM simulation software Sonnet [14] is used to perform the simulation.

### *B. Simulation and Measurement*

Fig. 11 shows the fabricated filter I with a size of 17.2 mm $\times$ 13.3 mm. Fig. 12 illustrates its simulated and measured responses. The measured results show that the filter has a center frequency of 1.015 GHz and two transmission zeros at 0.784 and 1.222 GHz. The measured passband insertion loss is approximately 3.1 dB, and the passband return loss is better than 16 dB. The first spurious response is at 5.631 GHz, and the rejection level is better than $-30$ dB from 1.116 to 5.364 GHz. The

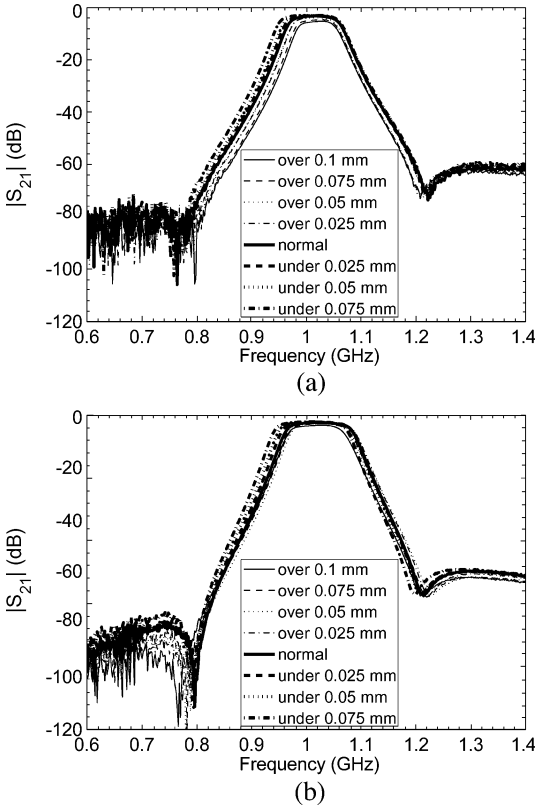


Fig. 15. Measured sensitivity to etching tolerances for the proposed SIR filter. (a) Filter I. (b) Filter II (over: over-etching; under: under-etching).

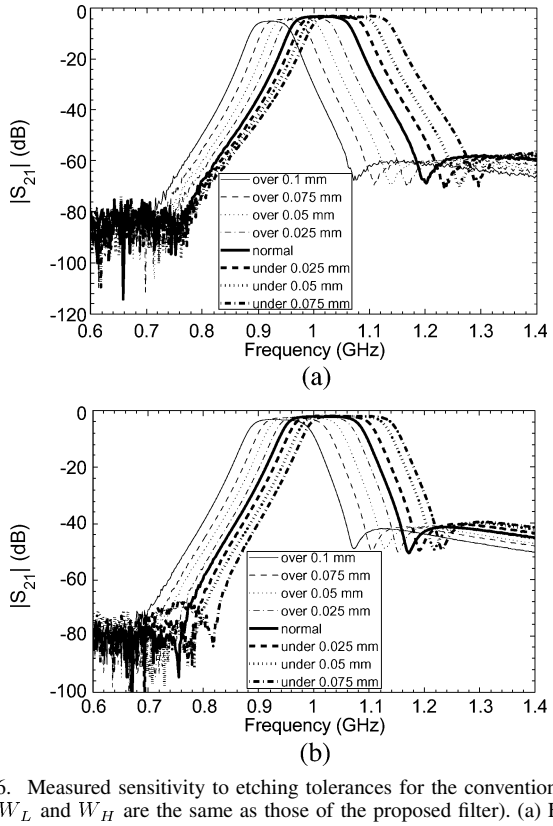


Fig. 16. Measured sensitivity to etching tolerances for the conventional SIR filter ($W_L$ and $W_H$ are the same as those of the proposed filter). (a) Filter I. (b) Filter II (over: over-etching; under: under-etching).

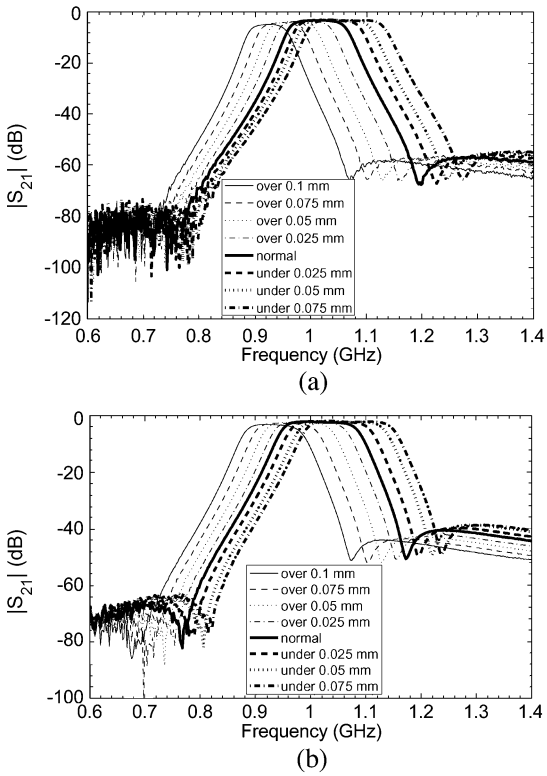


Fig. 17. Measured sensitivity to etching tolerances for the conventional SIR filter ($R$ and $W_H$ are the same as those of the proposed filter). (a) Filter I. (b) Filter II (over: over-etching; under: under-etching).

comparison between the simulated and measured results gives good agreement. For filter II, Fig. 13 shows a photograph of the fabricated circuit, which has a size of 17.7 mm × 13.5 mm. The simulated and measured responses of filter II are presented in Fig. 14. The measured results show that the filter has a center frequency of 1.023 GHz and two transmission zeros at 0.796 and 1.214 GHz. The measured passband insertion loss is approximately 2.2 dB, and the passband return loss is better than 15 dB. The first spurious frequency is at 5.085 GHz, which is a little down-shifted due to the resonance of the cross-coupling microstrip. The rejection level is better than −30 dB from 1.147 to 4.967 GHz.

It can be seen that both filters have symmetric insertion loss responses and sharp skirt characteristics. The insertion loss is mainly due to the conductor loss. Although a lot of via-holes are used in the proposed low-impedance microstrip structure, they have little effect on the passband insertion loss. This is because in the passband of the filter, the current is mainly distributed in the high-impedance section. There is little current through the via-holes on the inserted ground strips in the low-impedance section. Therefore, the loss is attributed to the high current density in the high-impedance section.

### *C. Sensitivity to Etching Tolerances*

To show the sensitivity to etching tolerances for the proposed SIR filters, we modify the masks during the fabrication process because PCB factories cannot change their processing parameters to match our study. Fig. 15 presents the measured responses of both proposed filters versus etching error, i.e., from over-etching 0.1 mm (4 mil) to under-etching 0.075 mm (3 mil), to demonstrate their sensitivity. Only the insertion loss curves

TABLE III
SENSITIVITY TO ETCHING TOLERANCES IN TERMS OF THE PERCENTAGE DEVIATION OF THE CENTER FREQUENCY FOR THE CONVENTIONAL AND PROPOSED SIR FILTERS

| | $\Delta f/f_0 \times 100$ (%)<br>$\Delta f$: the amount of center frequency drift<br>as. = as those of the proposed filter | over etching 0.1 mm | over etching 0.075 mm | over etching 0.05 mm | over etching 0.025 mm | normal | under etching 0.025 mm | under etching 0.05 mm | under etching 0.075 mm |
|---|---|---|---|---|---|---|---|---|---|
| Filter I | Proposed | 0.52 | 0.454 | -0.107 | 0.351 | 0 | -0.311 | -0.48 | -0.796 |
| | Conventional: the same $W_L$ and $W_H$ as. | -8.738 | -6.356 | -4.267 | -2.36 | 0 | 1.921 | 3.385 | 5.346 |
| | Conventional: the same $R$ and $W_H$ as. | -8.637 | -6.216 | -4.077 | -2.23 | 0 | 1.898 | 3.359 | 5.112 |
| Filter II | Proposed | -0.453 | 0.096 | 0.663 | 0.27 | 0 | -0.365 | -0.752 | -1.252 |
| | Conventional: the same $W_L$ and $W_H$ as. | -7.758 | -5.368 | -3.441 | -1.52 | 0 | 1.638 | 3.598 | 4.985 |
| | Conventional: the same $R$ and $W_H$ as. | -8.314 | -5.941 | -3.749 | -1.657 | 0 | 1.919 | 3.918 | 5.372 |

are shown for clarity. As observed in Fig. 15(a), the center frequency and two transmission zeros of filter I are almost unshifted in spite of inaccurate fabrication. The passband return losses, although not shown, are all better than 10 dB. The passband insertion loss and bandwidth are slightly changed. The passband insertion loss is higher for the over-etched case owing to the lower unloaded quality factor and narrower bandwidth. The bandwidth is wider for the under-etched case because the narrower gap results in the stronger coupling between the resonators. The same results are applied to filter II, as shown in Fig. 15(b), except the passband return losses are better than 12 dB in all cases.

The conventional $\lambda/4$ microstrip SIR filters were also designed and fabricated on the same substrates to compare with the proposed ones. The conventional SIR filters have the same center frequencies and bandwidths, as given in Table I, and similar layout configurations, as shown in Fig. 10, except that there is no inserted ground strip in the low-impedance section. We set two groups of parameters for comparison. The first group of the conventional SIR filters keeps the same dimensions $W_L$ and $W_H$ as those of the proposed SIR filters. The second group of the conventional SIR filters is designed with the same impedance ratio $R$ and width $W_H$ as those of the proposed SIR filters. Their measured responses versus etching error are shown in Figs. 16 and 17, respectively. Again, only the insertion loss curves are shown for both groups of filters. As expected from the figures for both groups of the conventional SIR filters, the center frequency and two transmission zeros are significantly shifted. The passband return losses of the conventional SIR filters, although not shown, are worse than those of the proposed ones when the etching error occurs. An extra benefit of the proposed SIR filters is that an obvious size reduction is achieved. For example, there is a size reduction of 39% for the proposed filter II compared with the conventional SIR filter when they have the same impedance ratio $R$ and width $W_H$. Table III summarizes the percentage of the center frequency drift due to etching errors for the proposed SIR filters and two groups of the conventional SIR filters. It can be clearly observed that the proposed $\lambda/4$ microstrip SIR filters show much less sensitivity to fabrication tolerances and have better performance.

## IV. CONCLUSION

A novel modified $\lambda/4$ microstrip SIR structure, which is tolerant to fabrication errors, has been presented in this paper. By inserting ground strips inside the low-impedance microstrip line, a new low-impedance transmission line, which makes the proposed SIR less sensitive to substrate thickness variations and etching tolerances, has been achieved. Moreover, the proposed microstrip SIR has shown an extra benefit of size reduction. Two four-pole cross-coupled filters with the proposed SIR structure have been realized with different amounts of etching error. The results have proven that the proposed filters have compact sizes, high selectivity, wide stopband range, and most importantly, insensitivity to fabrication inaccuracies.

## REFERENCES


[1] M. Makimoto and S. Yamashita, "Compact bandpass filters using stepped impedance resonators," *Proc. IEEE*, vol. 67, no. 1, pp. 16–19, Jan. 1979.

[2] M. Makimoto and S. Yamashita, "Bandpass filters using parallel coupled stripline stepped impedance resonators," *IEEE Trans. Microw. Theory Tech.*, vol. MTT-28, no. 12, pp. 1413–1417, Dec. 1980.

[3] M. Sagawa, M. Makimoto, and S. Yamashita, "A design method of bandpass filters using dielectric-filled coaxial resonators," *IEEE Trans. Microw. Theory Tech.*, vol. MTT-33, no. 2, pp. 152–157, Feb. 1985.

[4] Y. Qian, K. Yanagi, and E. Yamashita, "Characterization of a folded stepped-impedance resonator for miniature microstrip bandpass filter applications," in *Proc. 25th Eur. Microw. Conf.*, Bologna, Italy, Oct. 1995, vol. 2, pp. 1209–1211.

[5] M. Sagawa, M. Makimoto, and S. Yamashita, "Geometrical structures and fundamental characteristics of microwave stepped-impedance resonators," *IEEE Trans. Microw. Theory Tech.*, vol. 45, no. 7, pp. 1078–1085, Jul. 1997.

[6] S. Y. Lee and C. M. Tsai, "New cross-coupled filter design using improved hairpin resonators," *IEEE Trans. Microw. Theory Tech.*, vol. 48, no. 12, pp. 2482–2490, Dec. 2000.

[7] M. Makimoto and S. Yamashita, *Microwave Resonators and Filters for Wireless Communication: Theory, Design and Application*. Berlin, Germany: Springer-Verlag, 2001.

[8] J. T. Kuo and E. Shih, "Microstrip stepped impedance resonator bandpass filter with an extended optimal rejection bandwidth," *IEEE Trans. Microw. Theory Tech.*, vol. 51, no. 5, pp. 1554–1559, May 2003.

[9] C. F. Chen, T. Y. Huang, and R. B. Wu, "Compact microstrip cross-coupled bandpass filters using miniaturized stepped impedance resonators," in *Proc. Asia–Pacific Microw. Conf.*, Suzhou, China, Dec. 2005, vol. 1, pp. 493–496.

[10] S. C. Lin, P. H. Deng, Y. S. Lin, C. H. Wang, and C. H. Chen, "Wide-stopband microstrip bandpass filters using dissimilar quarter-wavelength stepped-impedance resonators," *IEEE Trans. Microw. Theory Tech.*, vol. 54, no. 3, pp. 1011–1018, Mar. 2006.

[11] A. Djaiz and A. Denidni, "A new compact microstrip two-layer bandpass filter using aperture-coupled SIR-hairpin resonators with transmission zeros," *IEEE Trans. Microw. Theory Tech.*, vol. 54, no. 5, pp. 1929–1936, May 2006.

[12] T. H. Huang, H. J. Chen, C. S. Chang, L. S. Chen, Y. H. Wang, and M. P. Houng, "A novel compact ring dual-mode filter with adjustable second-passband for dual-band applications," *IEEE Microw. Wireless Compon. Lett.*, vol. 16, no. 6, pp. 360–362, Jun. 2006.

[13] J. S. Wong, "Microstrip tapped-line filter design," *IEEE Trans. Microw. Theory Tech.*, vol. MTT-27, no. 1, pp. 44–50, Jan. 1979.

[14] *"Em User's Manual,"* Sonnet Softw., Liverpool, NY, 2004.

[15] *"Reference Guide Microwave Office,"* AWR, El Segundo, CA, 2003.
[16] M. Dishal, "Alignment and adjustment of synchronously tuned multiple-resonant-circuit filters," *Proc. IRE*, vol. 39, no. 11, pp. 1448–1455, Nov. 1951.
[17] J. S. Hong and M. J. Lancaster, *Microstrip Filters for RF/Microwave Applications*. New York: Wiley, 2001.
[18] J. S. Hong, E. P. McErlean, and B. M. Karyamapudi, "A high-temperature superconducting filter for future mobile telecommunication systems," *IEEE Trans. Microw. Theory Tech.*, vol. 53, no. 6, pp. 1976–1981, Jun. 2005.

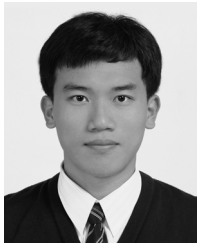

**Cheng-Hsien Liang** was born in Kaohsiung, Taiwan, on November 5, 1982. He received the B.S. and M.S. degrees in communication engineering from National Chiao-Tung University, Hsinchu, Taiwan, in 2005 and 2007, respectively, and is currently working toward the Ph.D. degree in communication engineering at National Chiao-Tung University.

His research interests include the analysis and design of microwave and millimeter-wave circuits.

**Chin-Hsiung Chen** was born in Taipei, Taiwan, on May 21, 1970. He received the B.S. degree in industrial education and technology from the National Changhua University of Education, Changhua, Taiwan, in 1994, the M.S. degree in engineering and system science from National Tsing-Hua University, Hsinchu, Taiwan, in 2001, respectively, and is currently working toward the Ph.D. degree in communication engineering from National Chiao-Tung University, Hsinchu, Taiwan.

His research interests include the analysis and design of microwave and millimeter-wave circuits.

**Chi-Yang Chang** (M'95) was born in Taipei, Taiwan, on December 20, 1954. He received the B.S. degree in physics and M.S. degree in electrical engineering from National Taiwan University, Taipei, Taiwan, in 1977 and 1982, respectively, and the Ph.D. degree in electrical engineering from The University of Texas at Austin, in 1990.

From 1990 to 1995, he was an Associate Researcher with the Chung-Shan Institute of Science and Technology (CSIST), where he was in charge of development of uniplanar circuits, ultra-broadband circuits, and millimeter-wave planar circuits. In 1995, he joined the faculty of the Department of Communication Engineering, National Chiao-Tung University, Hsinchu, Taiwan, as an Associate Professor, and became a Professor in 2002. His research interests include microwave and millimeter-wave passive and active circuit design, planar miniaturized filter design, and monolithic microwave integrated circuit (MMIC) design.